THE JOURNAL OF PHYSICAL CHEMISTRY B

pubs.acs.org/JPCB Article

Order and Disorder in ABCA′ Tetrablock Terpolymers

Madalyn R. Radlauer, Akash Arora, Megan E. Matta, Frank S. Bates, Kevin D. Dorfman,* and Marc A. Hillmyer*

Cite This: J. Phys. Chem. B 2020, 124, 10266−10275 Read Online

ACCESS | Metrics & More | Article Recommendations | Supporting Information

ABSTRACT: Self-assembly of poly(styrene)-*block*-poly(isoprene)-*block*-poly(lactide)-*block*-poly(styrene) (PS−PI−PLA−PS′ or SILS′) tetrablock terpolymers, where the volume fractions of the first three blocks are nearly equivalent, was studied both experimentally and using the self-consistent field theory (SCFT). SCFT indicates that addition of the terminal PS′ chain to a low-molecular-mass, hexagonally packed cylinders forming, SIL precursor can produce a disordered state due to preferential mixing of the polystyrene end-blocks with the PI and PLA midblocks in the SILS′ tetrablock, alleviating the unfavorable contact between the highly incompatible PI and PLA segments. In contrast, SCFT predicts that higher-molar-mass triblock precursors will maintain an ordered morphology upon addition of the terminal PS′ block due to stronger overall segregation strengths. These predictions were tested using three sets of SILS′ polymers that were synthesized based on three precursor SIL triblock polymers differing in total molar mass (14, 30, and 47 kg mol^{-1}) and varying the length of the terminal PS′ chain. In the lowest-molar-mass set of tetrablock polymers, the shift from order to disorder was observed in the materials at ambient temperature as the molar mass of the terminal PS′ block was increased, consistent with SCFT calculations. Disorder with longer S′ chain lengths was not found in the two higher-molar-mass polymer sets; the medium-molar-mass set showed both microphase separation and long-range order based on transmission electron microscopy (TEM) and small-angle X-ray scattering (SAXS), while the largest of these block polymers microphase separated but showed limited long-range order. The combination of the experimental and theoretical results presented in this work provides insights into the self-assembly of ABCA′-type polymers and highlights potential complications that arise from frustration in accessing well-ordered materials.

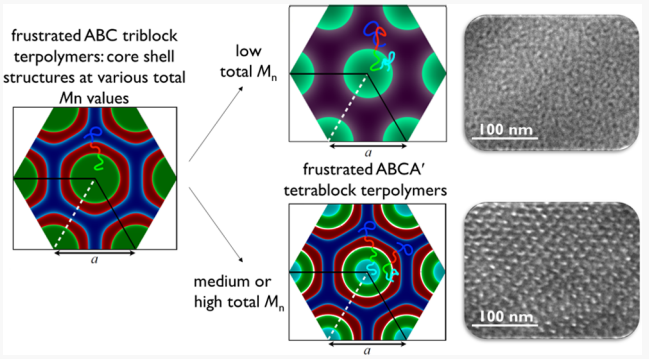

INTRODUCTION

The ability of block polymers consisting of covalently linked, chemically distinct blocks to self-assemble on the nanoscale results in hybrid materials that can enable a plethora of applications.[1] Multiblock polymers offer great potential for material design by incorporating multiple chemical functionalities with controlled localization of those functionalities at the nanoscale. This significant practical advantage is accompanied by a daunting engineering challenge, as the self-assembly of multiblock polymers is more difficult to predict and control than the well-studied diblock copolymers.[2] In the latter case, a straightforward analysis[3] of the competition between chain stretching and interfacial tension, as well as self-consistent field theory (SCFT),[4] leads to the emergence of three morphologies with an increasing volume fraction of the minority block: body-centered cubic (bcc) particles, hexagonally packed cylinders (hex), and a lamellar morphology (lam). The boundary between the hex and lam phases is interrupted by a co-continuous, double-gyroid network phase,[5] whose energetic basis is somewhat more complicated,[6−8] and a small region of another network morphology, the *Fddd* O^{70} phase, near to the order−disorder transition.[9,10]

While more complicated packings of particles can be obtained in diblock copolymers by increasing the conformational asymmetry of the blocks,[11,12] the number of possible morphologies available in a diblock copolymer remains relatively limited. In contrast, addition of a third block to form ABC triblock terpolymers greatly increases the number of possible morphologies.[13,14] The key new feature arising in a triblock terpolymer is the concept of frustration;[15,16] if the A/C mixing is more favorable than A/B or B/C mixing, the system becomes frustrated because the connectivity of the blocks enforces the enthalpically unfavorable A/B or B/C contacts. This effect is quantified by the Flory−Huggins parameter χ_{ij} between blocks i and j, where the frustrated system corresponds to $\chi_{AC} \ll \chi_{AB}$ or $\chi_{AC} \ll \chi_{BC}$. In addition to the scientific interest engendered by such triblock terpolymers,

Received: August 18, 2020
Revised: October 6, 2020
Published: November 2, 2020

https://dx.doi.org/10.1021/acs.jpcb.0c07543
J. Phys. Chem. B 2020, 124, 10266−10275

additional blocks also open up new opportunities for applications. For example, if the system is designed so that it creates a cylindrical morphology with an etchable terminal block, the remaining B block can impart a chemical functionality to the surfaces of the resulting nanoporous sample that could be useful, for example, in membrane separations.[17]

We are interested in the next level of complexity in multiblock polymers, namely, linear tetrablock terpolymers consisting of four blocks and three chemically distinct repeat units. Twenty years ago, some of the earliest screening of potential ABCA tetrablock terpolymer phase behavior with SCFT calculations revealed a variety of interesting morphologies, even in a nonfrustrated system.[18] There now exists a body of literature[19−25] on the self-assembly of ABAC and ABA′C tetrablock terpolymers for $\chi_{BC} \gg \chi_{AC} \approx \chi_{AB}$, where the prime notation indicates the same repeat unit but different block molar masses and thus volume fractions. This system is not frustrated because the highly unfavorable B/C interactions are limited by the presence of the A′ block. The "pseudo-diblock" system is a particularly interesting case where (i) the C block volume fraction is similar to the volume fraction of the minority block in an AB diblock and (ii) the composition is within the particle-forming part of the diblock phase diagram. The resulting tetrablock terpolymer system forms particles with cores of C organized within a matrix of A and B, creating the pseudo-diblock system. A positive value of χ_{AB} leads to structuring of that matrix, which then alters the balance between interfacial energy and chain stretching that would otherwise produce bcc ordering of the particles of C. The particle-forming region of the nonfrustrated tetrablock terpolymer system has been studied both experimentally, using poly(styrene)-*b*-poly(isoprene)-*b*-poly(styrene)′-*b*-poly(ethylene oxide) (SIS′O),[19,20] poly(cyclohexylethylene)-*b*-poly(ethylene)-*b*-poly(cyclohexylethylene)-*b*-poly(dimethylsiloxane),[21] and poly(styrene)-*b*-poly(isoprene)-*b*-poly(styrene)′-*b*-poly(2-vinylpyridine)[22] as model systems, and by SCFT for both experimental systems[19,23] and in more general cases.[24,25] Both experiments and theory produce a cornucopia of sphere-forming phases, most notably the emergence of a Frank−Kasper A15 phase that is stabilized by weak microphase separation of the matrix.[19]

In addition to the latter work on ABAC and ABA′C tetrablock terpolymers, there exists literature on other tetrablock terpolymer architectures. Both Monte Carlo simulations of ABCA polymers in solution[26,27] and SCFT calculations of ABCA polymers in the melt[28,29] suggest that non-centrosymmetric and Janus-type structures can be achieved by these polymers depending on the relative volume fractions and interaction parameters. Consistent with the theory, non-centrosymmetric structures have been observed experimentally for nonfrustrated ABCA polymers both in the melt and in aqueous media.[30,31] Vesicles and micelles formed in solutions of frustrated and nonfrustrated ABCA′ polymers have shown well-ordered, symmetric, microphase-separated structures.[32−34] While these works have revealed a wealth of information about the ordering of tetrablock terpolymers, the large state space of this system makes developing a relatively complete understanding of their phase behavior, akin to that achieved for conformationally symmetric diblock copolymers,[35] a significant challenge.

In the present contribution, we consider how the phase behavior of an otherwise ordered triblock terpolymer is affected by the addition of a fourth block, examining an ABCA′ tetrablock terpolymer synthesized from a frustrated parent ABC terpolymer ($\chi_{AC} \ll \chi_{AB}$ or $\chi_{AC} \ll \chi_{BC}$). As a model system, we use a parent triblock of poly(styrene)-*b*-poly(isoprene)-*b*-poly(lactide) (SIL) where the parent triblock has roughly equal volume fractions of each block.[36] This system is quite similar in its Flory−Huggins parameters to poly(styrene)-*b*-poly(isoprene)-*b*-poly(ethylene oxide) (SIO), where the poly(lactide) plays the role of the poly(ethylene oxide). Prior experimental work on this system[36] indicates that this SIL triblock polymer forms a hex phase, where the cylinder cores are poly(lactide) (PLA) with a shell of poly(isoprene) (PI) in a PS matrix. The cylinders are highly faceted owing to the polygonal nature of the intermaterial dividing surface.[37] Companion SCFT calculations[36] also produce a similarly faceted hex phase, but the predicted equilibrium morphology using literature-based estimates for the trio of Flory−Huggins parameters is a trilayer lam phase; the transition to a hex phase occurs at a lower ratio of χ_{AB}/χ_{BC} than is expected in experiments. The SIL system is attractive for our purposes since the chemistry required to convert these triblock terpolymers into SILS′ tetrablock terpolymers is robust (Figure 1).[38]

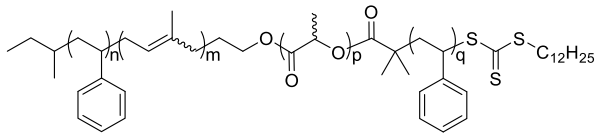

Figure 1. Polystyrene-block-polyisoprene-block-polylactide-block-polystyrene (SILS′) tetrablock terpolymers.

We examine here how the ordering of the initially hexagonally closed-packed cylindrical phase produced by SIL in the limit of equal volume fractions is impacted by the addition of a PS′ block of varying molar mass to form the tetrablock terpolymer in Figure 1. Prior experiments using the nonfrustrated SIS′O system have already demonstrated that the ordered phase behavior changes significantly upon addition of the terminal block;[39] our goal here is to examine the frustrated case and determine whether the frustration that leads to an ordered phase in the triblock terpolymer[36] can be relieved by conversion to a tetrablock terpolymer. We adopt first a theory-based approach, using SCFT to identify the circumstances under which the initially ordered SIL triblock terpolymer becomes disordered by the addition of the terminal PS′ block. Subsequent inspection of block volume fractions and total molar mass of the SIL triblock indicates that disorder emerges when the PS′ block of high molar mass is added to sufficiently low-molar-mass SIL triblock, owing to the mixing of PS′ and PLA in the matrix. However, if the parent triblock is of high molar mass, the added PS′ block loops back instead of mixing with PLA, thereby maintaining the ordered state. We then test these theoretical predictions using a set of three parent triblock polymers with total number-averaged molar masses of 14, 30, and 47 kg mol^{-1} at varying volume fractions of PS′ to PS. The qualitative predictions of SCFT are borne out by the lowest-molar-mass precursor, with a transition to disorder as the molar mass of the terminal PS′ block increases. Disorder with longer S′ chain lengths was not observed in the two higher-molar-mass polymer sets; the medium-molar-mass set showed both microphase separation and long-range order

https://dx.doi.org/10.1021/acs.jpcb.0c07543
J. Phys. Chem. B 2020, 124, 10266−10275

based on transmission electron microscopy (TEM) and small-angle X-ray spectroscopy (SAXS), while the largest-molar-mass set showed limited long-range order.

METHODS

Materials. Syntheses of the SIL and SILS′ triblock and tetrablock polymers via sequential anionic, ring-opening transesterification, and reversible addition−fragmentation chain-transfer polymerizations were described previously along with information on both sample preparation and characterization.[36,40] Molecular and thermal data on the polymers is included in the Supporting Information (Table S1).

Self-Consistent Field Theory Calculations. The calculations were performed using the open-source PSCF code,[41] following the methodology described in reference 36. The parameters for the SCFT calculations, based on the literature data for these blocks,[42−46] are outlined in the Supporting Information.

RESULTS AND DISCUSSION

Self-Consistent Field Theory. To focus our analysis, we examine the set of SIL triblock polymers with $M_{n,total}$ = 14, 30, and 47 kg mol^{-1} and consider cases where the additional PS block has a volume fraction given by the ratio $\xi = f_{S'}/f_S$. Figure 2 furnishes the full set of systems under consideration here. In

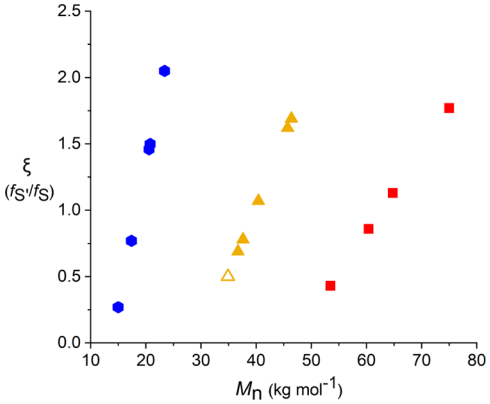

Figure 2. M_n of the entire tetrablock polymer versus ξ—the ratio of $f_{S'}$ to f_S—which quantifies the asymmetry of the two terminal polystyrene block lengths. The parent triblock polymer molar masses are 14 kg mol^{-1} (blue circles), 30 kg mol^{-1} (gold triangles), and 47 kg mol^{-1} (red squares); the polymers built from the same SIL triblock precursor are represented in the same color and shape. The solid data points are those that have been synthesized, while the open point represents a polymer composition analyzed by SCFT but not synthesized.

what follows, the notation SILS′_X$_\xi$ corresponds to a parent triblock with total number-averaged molar mass X (in kg mol^{-1}) with poly(styrene) block volume fraction ratio ξ (e.g., SILS′_47$_{1.8}$); the notation SILS′_X refers broadly to all tetrablock polymers formed from the parent triblock of molar mass X. The corresponding notation SIL_X refers to the parent triblock polymer.

To understand the role of adding a terminal PS′ block to a SIL precursor, it is useful to recall in some detail the SCFT predictions for the triblock polymer.[36] For the case where the volume fractions of each of the three blocks are approximately equal, SCFT calculations predict that the equilibrium morphology is a lamellar structure for the trio of Flory−Huggins parameters characterizing SIL over the temperature range of interest in experiments. It is only at relatively low values of χ_{SI}/χ_{IL} that the lam phase is overtaken by hex, consistent with the results of the strong-stretching theory for a generic ABC triblock system with equal volume fraction blocks.[47] It is not clear why the SCFT calculations fail to reproduce the experimentally observed hex morphology[36] as the equilibrium state, although possible reasons are uncertainties in the Flory−Huggins parameters,[23] molar mass and compositional dispersity,[48] or the finite molar mass of the polymers.[49]

In our investigation of the SILS′ system, we thus considered both lam and hex as ordered phases that compete against the disordered state; our primary goal is to determine whether the addition of the terminal PS′ block can stabilize a disordered phase against either of these ordered states, since the disagreement between the experiment and theory for the ordered phase in SIL has not been resolved.[36] We considered first the lowest-molar-mass triblock polymer SIL_14 and computed the free energies per chain of lam and hex relative to that of the disordered phase, $\Delta F/nk_BT$, as a function of volume fraction ($f_{S'}$) of the terminal PS′ block added to the SIL_14 triblock. These data are reported in Figure S1. At a given temperature, we look for the order−disorder transition temperature as a function of the terminal block volume fraction $f_{S'}$; with knowledge of the triblock molar mass, this volume fraction can be readily converted to a critical value $M^c_{S'}$ that must be added to the parent triblock to destabilize the ordered triblock terpolymer morphology. Note that, as the ordered structures move sufficiently far from their region of thermodynamic stability, their SCFT solutions no longer converge even when using a continuation method[41] to extend the previous solutions. In this case, we assume that the disordered state is preferred.

Figure 3 provides the critical value $M^c_{S'}$ for SILS′_14 tetrablocks formed from the smallest parent triblock polymer,

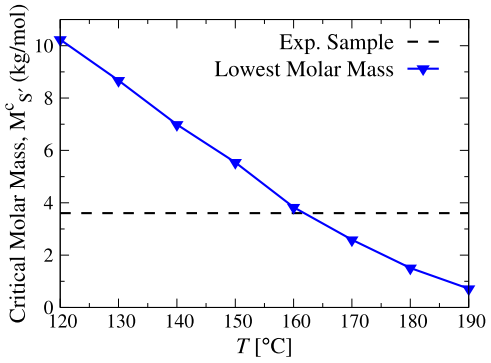

Figure 3. Minimum molar mass of the PS′ block that must be added to the parent SIL_14 triblock such that the resulting SILS′_14 tetrablock forms a disordered phase. These calculations were performed by considering lam and hex as the only ordered phase candidates. The segregation strengths as a function of temperature are calculated using the interaction parameters given in the SI.

SIL_14, over an experimentally realistic temperature range. To provide a concrete example, consider the system SILS′_14$_{0.77}$ in Figure 2. The molar mass of the terminal PS′ block is 3.6 kg mol^{-1}. The dashed line in Figure 3 indicates that this system should have an order−disorder transition temperature

https://dx.doi.org/10.1021/acs.jpcb.0c07543
J. Phys. Chem. B 2020, 124, 10266−10275

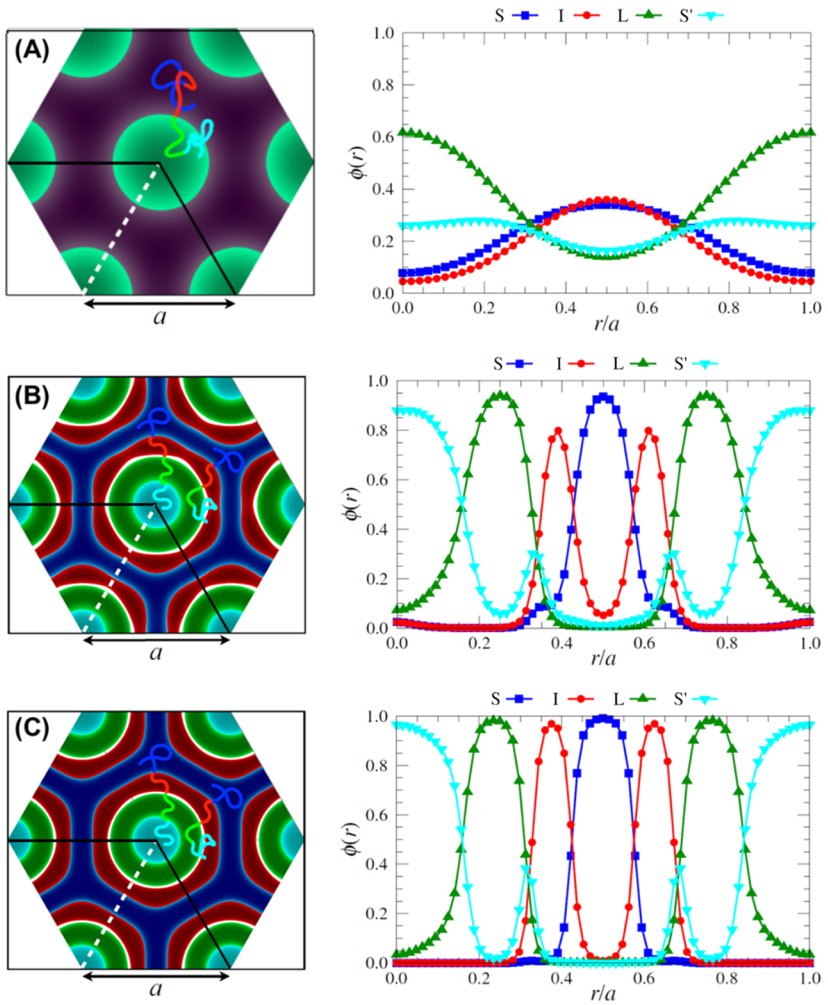

Figure 4. Density profiles from SCFT calculations of the cylinder morphology for SILS′ tetrablock terpolymers at T = 150 °C. Specifically, the segregation strengths ($\chi_{IS}N$, $\chi_{SL}N$, $\chi_{IL}N$) used are (a) (13.42, 14.91, 34.61), (b) (29.29, 32.55, 75.53), and (c) (45.91, 51.02, 118.40), and the volume fractions (f_S, f_I, f_L, $f_{S'}$) used are (a) (0.2731, 0.2651, 0.2530, 0.2088), (b) (0.2780, 0.2940, 0.2880, 0.1400), and (c) (0.2988, 0.3118, 0.2613, 0.1281). For SILS′_$14_{0.77}$ (A), mixing of the PS and PI blocks as well as of the PLA and PS′ blocks leads to disorder. Conversely, the PS′ blocks of SILS′_$30_{0.5}$ (B) and SILS′_$47_{0.86}$ (C) are predicted to loop back and ease frustration between the PI and PLA blocks, maintaining their ordered structures. The right panels provide the density profiles along the [11] direction, indicated by the dashed white lines in the left panels.

(ODT) of approximately 160 °C, since the molar mass of the terminal PS′ block exceeds the critical value $M^c_{S'}$ for $T \gtrsim 160$ °C (and thus produces a disordered state). Note that $M^c_{S'}$ should be a strong function of temperature, so that even at the lowest temperature (T = 120 °C), the molar mass of PS′ required to induce an ODT for a 14 kg/mol SIL triblock is only 10 kg/mol.

We also performed similar SCFT calculations for the higher-molar-mass precursors SIL_30 and SIL_47. We again only considered lam and hex structures for these samples, but even with this limited parameter space, the SCFT calculations predict that the tetrablock polymers will always form ordered structures within the temperature range 120 °C ≤ T ≤ 190 °C. Hence, there does not exist a critical $M^c_{S'}$ for the SILS′_30 and SILS′_47 polymers up to 190 °C. Clearly, these systems must exhibit an order−disorder transition at some higher temperature, and the location of the ODT will be influenced by the molar mass of the terminal PS′ block. We expect that it would be possible to form a disordered phase at any given temperature by adding a very long PS′ block, i.e., $f_{S'} \to 1$, leading to vanishingly small PI and PLA volume fractions. Under such conditions, even the SILS′_30 and SILS′_47 are predicted to collapse into a disordered phase. From this perspective, the transition from an ordered to a disordered phase by adding a terminal PS′ block is universal and should exist for any SIL triblock independent of its molar mass and temperature. Still, the $f_{S'} \to 1$ limit is impractical as it essentially creates a homopolymer of PS, and hence we restrict ourselves here to volume fractions $f_{S'} \leq 0.6$ in the final SILS′ tetrablock. Moreover, we restrict ourselves here to temperatures that can be feasibly studied in experiments without degradation of the polymers, as a SCFT prediction of an experimentally inaccessible ODT is not germane to our goals.

A particularly powerful aspect of SCFT for the tetrablock terpolymers is that it permits investigating the nanostructured morphology in ways that are challenging (or impossible) to do experimentally.[19,20,25] In the present circumstances, it is particularly illuminating to resolve the volume fractions of the PS and PS′ blocks to see how they are connected to the emergence of a disordered state in the tetrablock terpolymer as the volume fraction of the PS′ block is increased. To this end, Figure 4 shows the density profiles of different blocks within the cylindrical phase formed by SILS′_$14_{0.77}$, SILS′_$30_{0.50}$, and SILS′_$47_{0.86}$ tetrablock polymers at a temperature of T =

https://dx.doi.org/10.1021/acs.jpcb.0c07543
J. Phys. Chem. B 2020, 124, 10266−10275

150 °C. Density profiles for the corresponding parent SIL triblock polymers are provided in the Supporting Information (Figure S2). It is evident that the PS and PI blocks are intermixed significantly within the matrix for both SIL_14 (Figure S2) and SILS′_$14_{0.77}$ (Figure 4A). In contrast to the core−shell cylinder morphology observed for high-molar-mass SIL triblock terpolymers,[36] in SILS′_$14_{0.77}$, the cylinders are a mix of the PLA block and the terminal PS′ block (Figure 4A). Similarly, the first PS block mixes with the PI block to form the matrix around the cylinders. Such high degree of intermixing both in the matrix and in the core results from binary segregation strengths $\chi_{SI}N$ and $\chi_{LS}N$ for this sample that are not sufficiently high to segregate these blocks due to the low value of N. This preferential mixing of PS′ with PLA blocks is most likely the reason the disordered phase for the SILS′_14 polymers with longer PS′ blocks is observed.

In contrast to what happens with SILS′_14, SIL_30 and SILS′_$30_{0.50}$ form the well-segregated core−shell structures depicted by Figures S2B and 4B, respectively. Note that the SILS′ tetrablock in this case does not correspond directly to any of the experimentally synthesized samples because the calculation for the cylindrical phase for SILS′_$30_{0.69}$ (the smallest PS′ block used in experiments) failed to converge. Instead, Figure 4B represents a tetrablock with the maximum length of the terminal PS′ block possible where the cylindrical morphology would converge in SCFT, which is $M_{nS'}$ = 4.8 kg mol^{-1} (and thus SILS′_$30_{0.50}$). For SIL_30, the PLA block forms the core of the core−shell cylinder; however, for SILS′_$30_{0.50}$, the added PS′ block forms the core within a double shell of PLA and PI. In both the cases, the PI shell around the PLA block is faceted to maintain a constant density (incompressibility) of the melt. Another curious aspect of the density profile for SILS′_$30_{0.5}$ is that a noticeable amount of the PS′ block must loop back to form the thin region in between the PI and PLA blocks. This is probably a consequence of the frustration of the tetrablock based on the high binary segregation strength $\chi_{IL}N$; the PS′ block screens the interaction of PI from PLA, lowering the overall free energy of the system. Such looping back of the chains was also observed in work on the self-assembly of ABC bottlebrush triblock terpolymers.[50]

The tendency of the PS′ block to loop back amplifies for the higher-molar-mass sample, SILS′_$47_{0.86}$ (Figure 4C). The density of the PS′ block in between PI and PLA blocks is increased for SILS′_$47_{0.86}$ compared to SILS′_$30_{0.5}$ (Figure 3). Overall, SILS′_$47_{0.86}$ forms well-defined trilayer cylinders similar to SILS′_$30_{0.5}$ but with much sharper interfaces resulting from the extremely high value of $\chi_{IL}N$ in this frustrated system. Such significant frustration suggests that it may be difficult to achieve an equilibrium morphology experimentally for the SILS′_47 polymer set.

Experimental Results. We synthesized SILS′ polymers with a range of ξ values to provide comparisons to the SCFT results. Starting with the SIL_14 triblock polymer, which exhibited core−shell cylinder morphology seen in the TEM images of Figure 5A, and multiple peaks in the SAXS data indicating hexagonal packing (peaks in Figure 5B for SIL_14 include q^* = 0.270 nm^{-1}, $\sqrt{(3)}q^*$, and $\sqrt{(7)}q^*$), we performed chain extension by reversible addition−fragmentation chain-transfer (RAFT) polymerization to make the SILS′_14 polymers with ξ values going from 0.27 to 2.05. As expected from the computational results, two morphological consequences were observed. For the polymers with

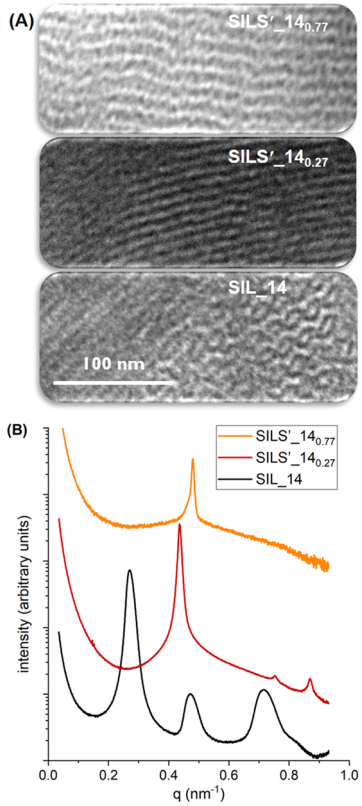

Figure 5. Representative TEM (A) and SAXS (B) data for the smallest triblock polymer and the two ordered tetrablock polymers made from this starting material: $M_{n,PS}$ = 4.7 kg mol^{-1}, $M_{n,PI}$ = 3.9 kg mol^{-1}, $M_{n,PLA}$ = 5.2 kg mol^{-1}, triblock (SIL_14, black, bottom), $M_{n,PS'}$ = 1.3 (SILS′_$14_{0.27}$, red), and 3.6 (SILS′_$14_{0.77}$, orange) kg mol^{-1}. These data were collected after thermally annealing the samples for 16 h at ∼120 °C. The TEM samples were vapor-stained with OsO_4. See Figure S5 for a TEM image of SILS′_$14_{0.27}$ stained with RuO_4.

shorter PS′ blocks, SILS′_$14_{0.27}$ and SILS′_$14_{0.77}$, layered structures were seen in the TEM images (Figure 5A), which are interpreted as the side-on view of hexagonally packed cylinders based on the peaks in the SAXS data in the case of SILS′_$14_{0.27}$ (Figure 5B, q^* = 0.437 nm^{-1}, $\sqrt{(3)}q^*$, and $\sqrt{(4)}q^*$). Morphological assignment for SILS′_$14_{0.77}$ could not be established based on the data presented in Figure 5, but some TEM images of this sample gave apparent layer spacings of about 8 nm, which could be associated with a projection of hexagonally packed cylinders with a principal spacing of 13 nm (q^* = 0.48 nm^{-1}). For the larger SILS′_14 materials, however, disordered materials were evident by both TEM and SAXS before and after annealing (Figures 6, S3, and S4).

At the annealing temperature of 120 °C, the SCFT predicts that disordered structures would be evident at larger PS′ block lengths (>10 kg mol^{-1}). For our synthesized materials with $M_{n,PS'}$ = 6.8−9.6 kg mol^{-1}, disorder is evident in both the TEM and SAXS results at ambient temperature. These systems demonstrate a physical manifestation of the SCFT results and are consistent with the PS blocks mixing with the PI and PLA blocks and alleviating the associated frustration of the system despite the PS blocks being positioned at the ends of the polymers.

SILS′_30 tetrablock terpolymers built from the SIL_30 triblock precursor achieved ordered structures regardless of the PS′ block length (ξ values ranging from 0.69 to 1.7), consistent

https://dx.doi.org/10.1021/acs.jpcb.0c07543
J. Phys. Chem. B 2020, 124, 10266−10275

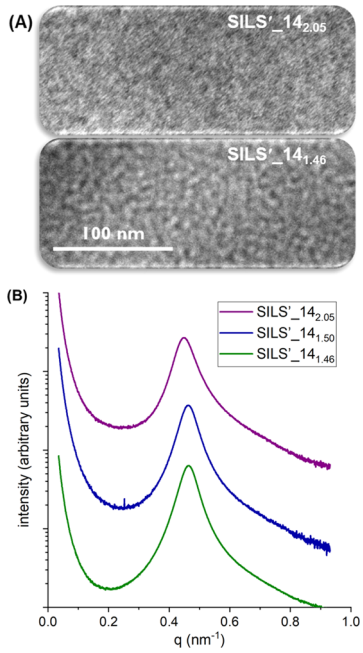

Figure 6. Representative TEM (A) and SAXS (B) of the disordered tetrablock polymers SILS′_14$_{1.46}$ ($M_{n,PS'}$ = 6.8 kg mol^{-1}, green), SILS′_14$_{1.50}$ ($M_{n,PS'}$ = 7.0 kg mol^{-1}, blue), and SILS′_14$_{2.05}$ ($M_{n,PS'}$ = 9.6 kg mol^{-1}, purple, top). The SAXS data were collected after thermally annealing the samples for 16 h at ∼120 °C, while the TEM images of SILS′_14$_{2.05}$ and SILS′_14$_{1.46}$ were acquired without thermal annealing. The TEM samples were vapor-stained with OsO_4. Additional TEM images of these polymers are shown in Figure S4.

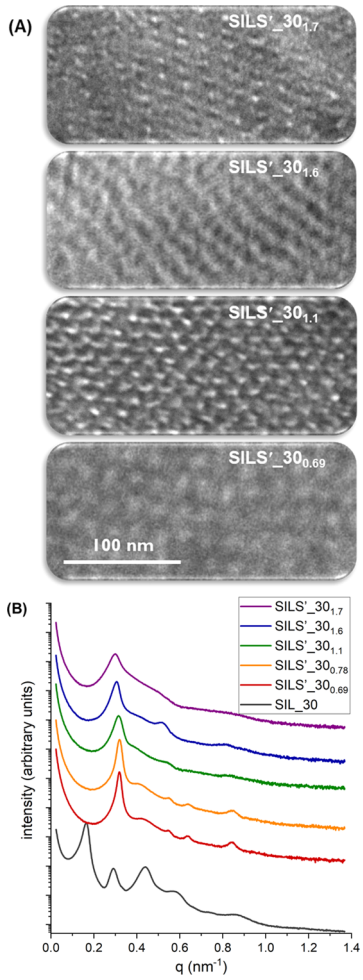

Figure 7. Representative TEM (A) and SAXS (B) data for the middle polymer set: $M_{n,PS}$ = 9.6 kg mol^{-1}; $M_{n,PI}$ = 8.7 kg mol^{-1}, $M_{n,PLA}$ = 12 kg mol^{-1}, $M_{n,PS'}$ = 6.6 (SILS′_30$_{0.69}$, red, bottom), 7.5 (SILS′_30$_{0.78}$, orange), 10.3 (SILS′_30$_{1.1}$, green), 15.5 (SILS′_30$_{1.6}$, blue), and 16.2 (SILS′_30$_{1.7}$, purple, top) kg mol^{-1}. These data were collected after thermally annealing the samples for 160 h at ∼120 °C. The TEM samples were vapor-stained with RuO_4. The TEM images of SILS′_30$_{0.78}$ were obtained without thermal annealing (Figure S6), but no clear images were obtained after thermal annealing.

with the SCFT results (Figure 7). Only a slight shift is observed in the primary SAXS peaks for the SILS′_30 tetrablock terpolymers, indicating similar domain sizes despite molar mass differences of up to 25%, though other peaks shifted to lower q values as the PS′ block was extended. The sharper peaks for SILS′_30$_{0.69}$, SILS′_30$_{0.78}$, and SILS′_30$_{1.1}$ are consistent with the hexagonal packing evident in the corresponding TEM images, though an additional broader peak exists as a shoulder to the right of each of the primary peaks that is not expected in hexagonal symmetry. The SAXS traces for the largest two SILS′_30 polymers with ξ values of 1.6 and 1.7 still have multiple features, though they are broader.

While ordered, frustrated, tetrablock terpolymers were accessed with the SILS′_30 series, neither the TEM images nor the SAXS data could provide a full picture of the morphology. For the TEM images in Figure 7, the samples were vapor-stained with RuO_4, which stains both PS and PI, so that the lighter domains are expected to be PLA. Unfortunately, areas that are PS and areas that are PI are not clearly defined by this staining method. Thus, a complementary staining experiment was completed with OsO_4, which should stain PI most heavily, PS lightly (if at all), and PLA not at all. Side-by-side comparison of the two samples with the complementary stains still does not provide a clear picture of the morphology (Figure 8). In addition, only lamellae and core−shell cylinders were calculated by SCFT and neither of these morphologies appears to match the collected data.

Chain extension of our largest triblock precursor, SIL_47, led to a clear microphase separation of blocks (Figure 9), though long-range order was not achieved. As shown previously,[36] the triblock terpolymer self-assembles to form hexagonally packed core−shell cylinders with long-range order, as clearly seen in the SAXS data (Figure 9B, the SIL data was indexed to hexagonal symmetry and TEM images confirmed the morphology in our previous report). Yet while the extremely high values of $\chi_{IL}N$ for the SILS′_47 set of polymers were expected to provide strong segregation, especially between the PI and PLA, which would force each polymer block into a relatively pure domain in the annealed material, it was also expected that reaching an equilibrium structure may be difficult to achieve. Indeed, these samples produced well-segregated structures both before and after annealing and displayed morphologies upon annealing with both square-packed (SILS′_47$_{0.86}$) and hexagonally packed (SILS′_47$_{1.8}$) domains of PI as observed by TEM (Figure 9A). Even after over 100 h of thermal annealing at 120 °C, the polymers did not display long-range order, as evidenced both in the broad SAXS peaks (Figure 9B) and in the TEM images (Figures 9A, and S7). A higher annealing temperature could not be used due to decomposition of the polymer observed by SEC.[36,38]

https://dx.doi.org/10.1021/acs.jpcb.0c07543
J. Phys. Chem. B 2020, 124, 10266−10275

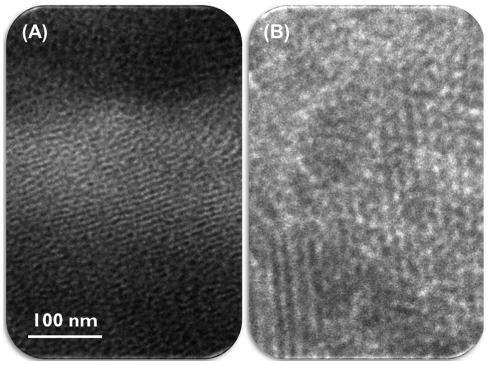

Figure 8. Complementary staining of the samples for TEM with OsO_4 (A) and RuO_4 (B) for SILS′_$30_{0.69}$. With OsO_4, the PI shows up as dark, while with the RuO_4, only the PLA shows up light, allowing us to discern the PI domain in the OsO_4-stained sample and the PLA in the RuO_4-stained sample. Unfortunately, the PS domain is not easy to distinguish in either because it appears similar to the PLA in the OsO_4-stained sample and similar to the PI in the RuO_4-stained sample.

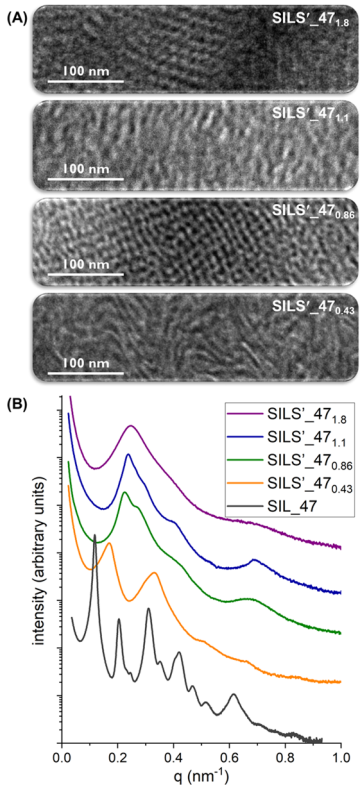

Figure 9. Representative TEM (A) and SAXS (B) data for the largest polymer set: $M_{n,PS}$ = 16 kg mol^{-1}; $M_{n,PI}$ = 14 kg mol^{-1}, $M_{n,PLA}$ = 17 kg mol^{-1}, $M_{n,PS'}$ = 6.8 (SILS′_$47_{0.43}$, orange, bottom), 14 (SILS′_$47_{0.86}$, green), 18 (SILS′_$47_{1.1}$, blue), or 28 (SILS′_$47_{1.8}$, purple, top) kg mol^{-1}. These data were collected after thermally annealing the samples for 112 h at ∼120 °C. The TEM samples were vapor-stained with OsO_4.

At shorter annealing times, different structures were evidenced by both TEM and SAXS (Figures S8 and S9), but clear long-range order was not observed. The SAXS data before and after annealing do appear to be related and the traces sharpen up after annealing (except in the case of SILS′_$47_{0.43}$), but the structures observed in the TEM images are not easily reconciled with one another. For example, SILS′_$47_{0.43}$ before annealing appears to be approaching a lamellar morphology, but after annealing, these domains appear more twisted and convoluted. Similarly, prior to annealing, SILS′_$47_{1.1}$ appears to present square-packed spheres or cylinders with a helical or stretched aspect, but the peaks in the SAXS trace are very broad. In contrast, the TEM image post annealing appears less ordered, though the SAXS peaks are starting to sharpen. Thus, it is unclear whether these represent structures that are along the pathway to long-range order.

Comparing the SILS′_14 polymers with the other two sets of materials confirms that there are thresholds for the calculated (dis)ordering behavior with respect to the degree of polymerization. Obtaining a disordered SILS′ tetrablock polymer by chain extension from an ordered SIL triblock polymer only occurs with the smallest tetrablock polymer set, despite accessing polymers with a significant total PS fraction in the SILS′_30 and SILS′_47 sets as well. As microphase separation is dependent on χN, a lower overall N is likely the predictive variable for this observation.

While the SCFT and experimental results are generally consistent, there is one notable difference. For all of the SILS′ tetrablock polymers, an increase in q^* was observed relative to the precursor triblock polymers, indicating a contraction of the domain spacing with the addition of the PS′ block. For example, the SAXS data show an increase in q^* from the SIL_47 triblock polymer to the SILS′_47 tetrablock polymers from 0.12 nm^{-1} to between 0.17 and 0.25 nm^{-1} (Figure 9B). This is contrary to the decrease in q^* going from SI to SIL (0.30 to 0.12 nm^{-1}), which is in accord with the common finding that an increase in overall polymer size is accompanied by an increase in domain size and spacing. These trends in q^* are not directly explained by the SCFT calculations, as the calculations predict an increase in the domain spacing from SIL to SILS′ (Table S3). Though changes in polymer architecture have been associated with a reduction of domain spacing,[51] previously published experimental and theoretical papers on the ABCA polymers generally do not compare domain spacing of the triblock and tetrablock polymers.[18,26−34]

It has been shown in the literature that the domain spacing of the frustrated ABC triblock polymers is a function of the added terminal block and can lead to a lower value by the addition of a terminal block.[52,53] For ABC triblock polymers, Xie et al. have demonstrated that the terminal C block forming the core can be in the relaxed coiled state in the core, but when a B block is added to form ABCB tetrablock polymers, the C block experiences appreciable stretching as both junctions are forced to the B/C interface.[52] To minimize such an increased stretching, the core of the C block shrinks, leading to a smaller domain spacing compare to that in the corresponding ABC triblock polymers. Such a behavior could also be happening in the SILS′ tetrablock polymers, but a key distinction here is that the terminal PS′ block forms the core, as opposed to the ABCB system in which the C block forms the core. This leads to two primary differences in comparison to the ABCB system of Xie et al.: (1) the PS′ block forming the core can still be in the relaxed state, so increasing the polymer length should increase the domain spacing and (2) the PLA block forms a concentric core around the PS′ block (Figure 3B,C) with two interfaces on either side, which can lead to much more stretching of the PLA block compared to that of the C block in the ABCB system. Cumulatively, these two opposing factors might lead to a decrease in the domain spacing, but the effect is expected to

https://dx.doi.org/10.1021/acs.jpcb.0c07543
J. Phys. Chem. B 2020, 124, 10266−10275

diminish as the length of the PLA block or the overall molar mass of the SILS′ tetrablock increases. Hence, this peculiar, experimentally observed contraction in the domain spacing for all of the tetrablock polymers considered here, especially for the higher-molar-mass polymers, remains an interesting open question for further investigation.

While the SCFT calculations do not account for the increase in q^* with the addition of a terminal S′ block, we believe that the results depicted in Figure 4 point to the reasons for this effect. SIL is a frustrated triblock polymer, whereby the unavoidable PI−PLA interfaces are energetically more unfavorable than the PS−PI interfaces. The compositionally symmetric SIL triblock molecular architecture constrains the associated morphology to a cylindrical geometry with a PLA core. Addition of the PS′ block at the end of the PLA block provides a mechanism for partially alleviating this packing frustration, as revealed in Figure 4B,C. Although a majority of the S′ block segregates to the core of the cylinders, a nontrivial fraction penetrates the PLA domain and wets the PLA−PI interface, which will significantly reduce the associated interfacial tension and alleviate the frustration of the system. Adding a larger S′ block offers greater configurational freedom in this regard. This in turn is likely to drive a transition to different morphologies, with smaller domain and ordered state dimensions, since a smaller interfacial tension shifts the balance between interfacial area and chain stretching toward increased interfacial area per polymer chain that can be accompanied by reduced chain stretching.

While we are not able to identify specific ordered state morphologies with the addition of S′ blocks, both SAXS and TEM are consistent with changes in structure in all three systems examined. Application of SCFT requires specification of a morphological symmetry, which we do not know for the SILS′ tetrablock terpolymers. Nevertheless, the insights provided by Figure 4, specifically interfacial wetting by the S′ blocks, substantiate our interpretation of the experiments. Recently reported work on ABCA′ tetrablock terpolymers demonstrates the formation of several new morphologies, including Janus spheres and cylinders as well as a helical supercylinder structure in which the B and C blocks form helices and twist with each other to form a supercylinder.[54] These morphologies could be forming in our SILS′ tetrablock terpolymers, especially in between the HEX and disordered phases. Considering all of these complex structures, in light of the experimental results presented in this manuscript, is certainly an interesting opportunity for future study.

CONCLUSIONS

Experimental and theoretical studies of three sets of frustrated ABCA′ polymers of relatively low molar mass (the largest tetrablock polymer had $M_{n,total}$ = 75.0 kg mol^{-1}) demonstrated unexpected difficulty in observing long-range order and well-defined structures. SCFT calculations showed that chain extension of an ABC triblock polymer to form an ABCA′ tetrablock polymer could result in disordering of the entire system, but only for smaller triblock parents with larger A′ blocks. This result was consistent with the experimental results where the smallest SILS′_14 polymers became disordered with larger PS′ blocks, while SILS′ polymers starting from larger SIL triblock polymer precursors adopted microphase-separated structures regardless of PS′ block size. The middle polymer set, SILS′_30, demonstrated achievable long-range order, even with relatively short polymer blocks of 6.6 to 16.2 kg mol^{-1}, while for the largest set of polymers, SILS′_47, long-range order was not achieved based on the broad SAXS traces, though intriguing patterns were observed in the TEM images.

SCFT on SILS′_$30_{0.5}$ and SILS′_$47_{0.86}$ indicated that frustration in these materials could be alleviated by having some of the PS′ blocks loop back in between the PI and PLA blocks, but that this mixing of the PS′ block does not result in disordered structures like those seen with the smallest tetrablock polymer set. Because density profiles were only calculated for the cylindrical phase of both of these polymers, it is unclear if the formation of a barrier occurs in the observed structures, or if noncylindrical morphologies are achieved that do not require this alleviation of frustration. Indeed, though the sharper peaks in the SAXS data for the SILS′_30 polymers do correspond to hexagonal packing, the TEM images display what could be a basket weave (for SILS′_$30_{1.1}$) or segmented lamellae (for SILS′_$30_{1.7}$ and SILS′_$30_{1.6}$). Even with complementary staining techniques (using OsO_4 or RuO_4), a clear picture that distinguishes between all three polymer types was not achieved. Still, the morphologies exhibited by the SILS′_30 polymers begin to deliver on the promise of new structures from ABCA′ tetrablock terpolymers.

ASSOCIATED CONTENT

Supporting Information

The Supporting Information is available free of charge at https://pubs.acs.org/doi/10.1021/acs.jpcb.0c07543.

Table of data on polymers including M_n, M_w, Đ, f_n, ξ, and T_g from ^{1}H NMR spectroscopy, size-exclusion chromatography, and differential scanning calorimetry; methods section; SCFT parameters; additional SCFT results including domain spacings, free-energy calculations, and density profiles; additional TEM images and SAXS traces after solvent casting and various extents of thermal annealing (PDF)

AUTHOR INFORMATION

Corresponding Authors

Kevin D. Dorfman − *Department of Chemical Engineering and Materials Science, University of Minnesota, Minneapolis, Minnesota 55455, United States;* orcid.org/0000-0003-0065-5157; Email: dorfman@umn.edu

Marc A. Hillmyer − *Department of Chemistry, University of Minnesota, Minneapolis, Minnesota 55455, United States;* orcid.org/0000-0001-8255-3853; Email: hillmyer@umn.edu

Authors

Madalyn R. Radlauer − *Department of Chemistry, University of Minnesota, Minneapolis, Minnesota 55455, United States; Department of Chemistry, San José State University, San José, California 95192, United States;* orcid.org/0000-0002-3226-5340

Akash Arora − *Department of Chemical Engineering and Materials Science, University of Minnesota, Minneapolis, Minnesota 55455, United States*

Megan E. Matta − *Department of Chemistry, University of Minnesota, Minneapolis, Minnesota 55455, United States;* orcid.org/0000-0002-9999-3107

Frank S. Bates − *Department of Chemical Engineering and Materials Science, University of Minnesota, Minneapolis,*

https://dx.doi.org/10.1021/acs.jpcb.0c07543
J. Phys. Chem. B 2020, 124, 10266−10275

Minnesota 55455, United States; orcid.org/0000-0003-3977-1278

Complete contact information is available at: https://pubs.acs.org/10.1021/acs.jpcb.0c07543

Notes

The authors declare no competing financial interest.

■ ACKNOWLEDGMENTS

This work was supported by the National Science Foundation (DMR-1333669 and DMR-1725272). During the bulk of this work, M.R.R. held the Camille and Henry Dreyfus Foundation Postdoctoral Fellowship in Environmental Chemistry. *rac*-Lactide was generously provided by Ortec. Parts of this work were carried out in the Characterization Facility, University of Minnesota, which receives partial support from NSF through the MRSEC program. SAXS data were obtained at the DuPont−Northwestern−Dow Collaborative Access Team (DND-CAT) located at Sector 5 of the Advanced Photon Source, a U. S. Department of Energy (DOE) Office of Science user facility operated for the DOE Office of Science by the Argonne National Laboratory under Contract No. DE-AC02-06CH11357. SCFT calculations were performed using the computational resources provided by the Minnesota Supercomputing Institute at the University of Minnesota.

■ REFERENCES

(1) Epps, T. H., III; O'Reilly, R. K. Block Copolymers: Controlling Nanostructure to Generate Functional Materials - Synthesis, Characterization, and Engineering. *Chem. Sci.* **2016**, *7*, 1674−1689.
(2) Bates, F. S.; Hillmyer, M. A.; Lodge, T. P.; Bates, C. M.; Delaney, K. T.; Fredrickson, G. H. Multiblock Polymers: Panacea or Pandora's Box? *Science* **2012**, *336*, 434−440.
(3) Bates, F. S.; Fredrickson, G. H. Block Copolymers − Designer Soft Materials. *Phys. Today* **1999**, *52*, 32−38.
(4) Leibler, L. Theory of Microphase Separation in Block Copolymers. *Macromolecules* **1980**, *13*, 1602−1617.
(5) Hajduk, D. A.; Harper, P. E.; Gruner, S. M.; Honeker, C. C.; Kim, G.; Thomas, E. L.; Fetters, L. J. The Gyroid: A New Equilibrium Morphology in Weakly Segregated Diblock Copolymers. *Macromolecules* **1994**, *27*, 4063−4075.
(6) Matsen, M. W.; Schick, M. Stable and Unstable Phases of a Diblock Copolymer Melt. *Phys. Rev. Lett.* **1994**, *72*, 2660−2663.
(7) Matsen, M. W.; Bates, F. S. Origins of Complex Self-Assembly in Block Copolymers. *Macromolecules* **1996**, *29*, 7641−7644.
(8) Cochran, E. W.; Garcia-Cervera, C. J.; Fredrickson, G. H. Stability of the Gyroid Phase in Diblock Copolymers at Strong Segregation. *Macromolecules* **2006**, *39*, 2449−2451.
(9) Tyler, C. A.; Morse, D. C. Orthorhombic Fddd Network in Triblock and Diblock Copolymer Melts. *Phys. Rev. Lett.* **2005**, *94*, No. 208302.
(10) Takenaka, M.; Wakada, T.; Akasaka, S.; Nishitsuji, S.; Saijo, K.; Shimizu, H.; Kim, M. I.; Hasegawa, H. Orthorhombic *Fddd* Network in Diblock Copolymer Melts. *Macromolecules* **2007**, *40*, 4399−4402.
(11) Lee, S.; Bluemle, M. J.; Bates, F. S. Discovery of a Frank-Kasper σ Phase in Sphere-Forming Block Copolymer Melts. *Science* **2010**, *330*, 349−353.
(12) Liu, M.; Qiang, Y.; Li, W.; Qiu, F.; Shi, A.-C. Stabilizing the Frank-Kasper Phases via Binary Blends of AB Diblock Copolymers. *ACS Macro Lett.* **2016**, *5*, 1167−1171.
(13) Meuler, A. J.; Hillmyer, M. A.; Bates, F. S. Ordered Network Mesostructures in Block Polymer Materials. *Macromolecules* **2009**, *42*, 7221−7250.
(14) Xu, W.; Jiang, K.; Zhang, P.; Shi, A.-C. A Strategy to Explore Stable and Metastable Ordered Phases of Block Copolymers. *J. Phys. Chem. B* **2013**, *117*, 5296−5305.
(15) Zheng, W.; Wang, Z.-G. Morphology of ABC Triblock Copolymers. *Macromolecules* **1995**, *28*, 7215−7223.
(16) Liu, M.; Li, W.; Qiu, F.; Shi, A. C. Theoretical Study of Phase Behavior of Frustrated ABC Linear Triblock Copolymers. *Macromolecules* **2012**, *45*, 9522−9530.
(17) Rzayev, J.; Hillmyer, M. A. Nanoporous Polystyrene Containing Hydrophilic Pores from an ABC Triblock Copolymer Precursor. *Macromolecules* **2005**, *38*, 3−5.
(18) Drolet, F.; Fredrickson, G. H. Combinatorial Screening of Complex Block Copolymer Assembly with Self-Consistent Field Theory. *Phys. Rev. Lett.* **1999**, *83*, 4317−4320.
(19) Chanpuriya, S.; Kim, K.; Zhang, J.; Lee, S.; Arora, A.; Dorfman, K. D.; Delaney, K. T.; Fredrickson, G. H.; Bates, F. S. Cornucopia of Nanoscale Ordered Phases in Sphere-Forming Tetrablock Terpolymers. *ACS Nano* **2016**, *10*, 4961−4972.
(20) Zhang, J.; Sides, S.; Bates, F. S. Ordering of Sphere Forming SISO Tetrablock Terpolymers on a Simple Hexagonal Lattice. *Macromolecules* **2012**, *45*, 256−265.
(21) Bluemle, M. J.; Fleury, G.; Lodge, T. P.; Bates, F. S. The O52 Network by Molecular Design: CECD Tetrablock Terpolymers. *Soft Matter* **2009**, *5*, 1587−1590.
(22) Miyamori, Y.; Suzuki, J.; Takano, A.; Matsushita, Y. Periodic and Aperiodic Tiling Patterns from a Tetrablock Terpolymer System of the A_1BA_2C Type. *ACS Macro Lett.* **2020**, *9*, 32−37.
(23) Arora, A.; Pillai, N.; Bates, F. S.; Dorfman, K. D. Predicting the Phase Behavior of ABAC Tetrablock Terpolymers: Sensitivity to Flory−Huggins Interaction Parameters. *Polymer* **2018**, *154*, 305−314.
(24) Khadilkar, M. R.; Paradiso, S. P.; Delaney, K. T.; Fredrickson, G. H. Inverse Design of Bulk Morphologies in Multiblock Polymers Using Particle Swarm Optimization. *Macromolecules* **2017**, *50*, 6702−6709.
(25) Liu, M.; Li, W.; Qiu, F.; Shi, A.-C. Stability of the Frank-Kasper σ-Phase in BABC Linear Tetrablock Terpolymers. *Soft Matter* **2016**, *12*, 6412−6421.
(26) Cui, J.; Jiang, W. Structure of ABCA Tetrablock Copolymer Vesicles and Their Formation in Selective Solvents: A Monte Carlo Study. *Langmuir* **2011**, *27*, 10141−10147.
(27) Ma, J.; Cui, J.; Han, Y.; Jiang, W.; Sun, Y. Monte Carlo Study of the Micelles Constructed by ABCA Tetrablock Copolymers and Their Formation in A-Selective Solvents. *RSC Adv.* **2015**, *5*, 86473−86484.
(28) Kaga, M.; Ohta, T. Dynamical Approach to Microphase Separation in ABCA-Type Tetrablock Copolymers. *J. Phys. Soc. Jpn.* **2006**, *75*, No. 043002.
(29) Liu, D.; Wang, Y.-Y.; Sun, Y.-C.; Han, Y.-Y.; Cui, J.; Jiang, W. Self-Assembly Behavior of Symmetrical Linear ABCA Tetrablock Copolymer: A Self-Consistent Field Theory Study. *Chin. J. Polym. Sci* **2018**, *36*, 888−896.
(30) Takano, A.; Soga, K.; Suzuki, J.; Matsushita, Y. Non-centrosymmetric Structure from a Tetrablock Quarterpolymer of the ABCA Type. *Macromolecules* **2003**, *36*, 9288−9291.
(31) Gomez, E. D.; Rappl, T. J.; Agarwal, V.; Bose, A.; Schmutz, M.; Marques, C. M.; Balsara, N. P. Platelet Self-Assembly of an Amphiphilic A−B−C−A Tetrablock Copolymer in Pure Water. *Macromolecules* **2005**, *38*, 3567−3570.
(32) Brannan, A. K.; Bates, F. S. ABCA Tetrablock Copolymer Vesicles. *Macromolecules* **2004**, *37*, 8816−8819.
(33) Hoogenboom, R.; Wiesbrock, F.; Leenen, M. A. M.; Thijs, H. M. L.; Huang, H.; Fustin, C.-A.; Guillet, P.; Gohy, J.-F.; Schubert, U. S. Synthesis and Aqueous Micellization of Amphiphilic Tetrablock Ter-and Quarterpoly(2-Oxazoline)s. *Macromolecules* **2007**, *40*, 2837−2843.
(34) Constantinou, A. P.; Sam-Soon, N. F.; Carroll, D. R.; Georgiou, T. K. Thermoresponsive Tetrablock Terpolymers: Effect of Architecture and Composition on Gelling Behavior. *Macromolecules* **2018**, *51*, 7019−7031.
(35) Khandpur, A. K.; Förster, S.; Bates, F. S.; Hamley, I. W.; Ryan, A. J.; Bras, W.; Almdal, K.; Mortensen, K. Polyisoprene-Polystyrene Diblock Copolymer Phase Diagram Near the Order-Disorder Transition. *Macromolecules* **1995**, *28*, 8796−8806.

(36) Radlauer, M. R.; Sinturel, C.; Asai, Y.; Arora, A.; Bates, F. S.; Dorfman, K. D.; Hillmyer, M. A. Morphological Consequences of Frustration in ABC Triblock Polymers. *Macromolecules* **2017**, *50*, 446−458.
(37) Stadler, R.; Auschra, C.; Beckmann, J.; Krappe, U.; Voight-Martin, I.; Leibler, L. Morphology and Thermodynamics of Symmetric Poly(A-block-B-block-C) Triblock Copolymers. *Macromolecules* **1995**, *28*, 3080−3097.
(38) Radlauer, M. R.; Fukuta, S.; Matta, M. E.; Hillmyer, M. A. Controlled Synthesis of ABCA′ Tetrablock Terpolymers. *Polymer* **2017**, *124*, 60−67.
(39) Bluemle, M. J.; Zhang, J.; Lodge, T. P.; Bates, F. S. Inverted Phases Induced by Chain Architecture in ABAC Tetrablock Terpolymers. *Macromolecules* **2010**, *43*, 4449−4452.
(40) Poelma, J. E.; Ono, K.; Miyajima, D.; Aida, T.; Satoh, K.; Hawker, C. J. Cyclic Block Copolymers for Controlling Feature Sizes in Block Copolymer Lithography. *ACS Nano* **2012**, *6*, 10845−10854.
(41) Arora, A.; Qin, J.; Morse, D. C.; Delaney, K. T.; Glenn, H.; Bates, F. S.; Dorfman, K. D. Broadly Accessible SCFT for Block Polymer Materials Discovery. *Macromolecules* **2016**, *49*, 4675−4690.
(42) Medapuram, P. Investigation of Universal Behavior in Symmetric Diblock Copolymer Melts. Ph.D. Thesis; University of Minnesota, 2015.
(43) Sinturel, C.; Bates, F. S.; Hillmyer, M. A. High χ−Low N Block Polymers: How Far Can We Go? *ACS Macro Lett.* **2015**, *4*, 1044−1050.
(44) Fetters, L.; Lohse, D.; Richter, D.; Witten, T.; Zirkel, A. Connection between Polymer Molecular Weight, Density, Chain Dimensions, and Melt Viscoelastic Properties. *Macromolecules* **1994**, *27*, 4639−4647.
(45) Eitouni, H. B.; Balsara, N. P. *Physical Properties of Polymers Handbook*; Springer, 2007; pp 339−356.
(46) Lee, S.; Gillard, T. M.; Bates, F. S. Fluctuations, Order, and Disorder in Short Diblock Copolymers. *AIChE J.* **2013**, *59*, 3502−3513.
(47) Lyatskaya, Y. V.; Birshtein, T. M. Triblock Copolymers: The Role of Interfacial Tension at Two Interfaces. *Polymer.* **1995**, *36*, 975−980.
(48) Jiang, Y.; Yan, X.; Liang, H.; Shi, A.-C. Effect of Polydispersity on the Phase Diagrams of Linear ABC Triblock Copolymers in Two Dimension. *J. Phys. Chem. B* **2005**, *109*, 21047−21055.
(49) Matsen, M. W. Self-Consistent Field Theory for Melts of Low-Molecular-Weight Diblock Copolymer. *Macromolecules* **2012**, *45*, 8502−8509.
(50) Chang, A. B.; Bates, C. M.; Lee, B.; Garland, C. M.; Jones, S. C.; Spencer, R. K.; Matsen, M. W.; Grubbs, R. H. Manipulating the ABCs of Self-Assembly via Low-χ Block Polymer Design. *Proc. Natl. Acad. Sci. U.S.A.* **2017**, *114*, 6462−6467.
(51) Poelma, J. E.; Ono, K.; Miyajima, D.; Aida, T.; Satoh, K.; Hawker, C. J. Cyclic Block Copolymers for Controlling Feature Sizes in Block Copolymer Lithography. *ACS Nano* **2012**, *6*, 10845−10854.
(52) Xie, N.; Liu, M.; Deng, H.; Li, W.; Qiu, F.; Shi, A. C. Macromolecular Metallurgy of Binary Mesocrystals via Designed Multiblock Terpolymers. *J. Am. Chem. Soc.* **2014**, *136*, 2974−2977.
(53) Duan, C.; Zhao, M.; Qiang, Y.; Chen, L.; Li, W.; Qiu, F.; Shi, A. C. Stability of Two-Dimensional Dodecagonal Quasicrystalline Phase of Block Copolymers. *Macromolecules* **2018**, *51*, 7713−7721.
(54) Xie, Q.; Qiang, Y.; Zhang, G.; Li, W. Emergence and Stability of Janus-Like Superstructures in an ABCA Linear Tetrablock Copolymer. *Macromolecules* **2020**, *53*, 7380−7388.

https://dx.doi.org/10.1021/acs.jpcb.0c07543
J. Phys. Chem. B 2020, 124, 10266−10275